JOURNAL OF PROPULSION AND POWER
Vol. 10, No. 3, May–June 1994

Injection of Bubbling Liquid Jets from Multiple Injectors into a Supersonic Stream

Takakage Arai* and Joseph A. Schetz†
Virginia Polytechnic Institute and State University, Blacksburg, Virginia 24061

Multiple (12 injectors) bubbling liquid jets (helium microbubbles in water) were injected transverse to a $M = 2.4$ airflow. Penetration and spray plume spreading angle were measured directly using nanoshadowgraphs and front-lighted pictures, respectively. The experiments were performed at two conditions, i.e., the constant supply pressure condition and the constant liquid mass flow rate condition. For the case of a parallel arrangement of the injector orifices to the airflow, the penetration of the jet array increased steadily from front to back. The last jet (12th jet) has over 5 times the penetration of the first jet for the water only case. The usual similarity law for the penetration, $h \propto \bar{q}^{0.5}$, was approximately valid also for the multiple water-only jets. For the bubbling jet case, the penetration of the first jet doesn't change with increasing gas concentration γ, but the rear jets have less penetration height than that of liquid-only jets at the constant injection pressure condition. For the constant injection pressure condition, the resulting penetration of the jet plume decreased with increasing γ. On the other hand, for the constant liquid mass flow rate condition, the penetration of the multiple bubbling jets increased a little with increasing γ. Straight coherent jets just coming out of orifice were observed for the $\gamma = 0$ case. Conical jet plumes were obtained for the bubbling jet case. Therefore, the width of the jet plume increased by using the bubbling jet. The effects of the angle between the orifice array and the freestream direction and the surfactant concentration on the penetration and mixing of multiple bubbling jets were also clarified.

Nomenclature

A	=	area of orifice
d	=	injector diameter
h	=	penetration of jet plume
M	=	Mach number
$\dot{m}$	=	mass flow rate
P	=	pressure
q	=	momentum
$\bar{q}$	=	jet to freestream momentum ratio, q_j/q_∞
$\bar{q}_l$	=	$\dot{m}_l^2/(A^2\rho_l)/q_\infty$
x, y, z	=	rectangular coordinates, origin at injector
α	=	spray plume spreading angle
γ	=	gas concentration, ratio of mass flow rate, $\dot{m}_g/\dot{m}_l$
θ	=	flow angle
ρ	=	density

Subscripts

g	=	gas
j	=	jet or mixture
l	=	liquid
∞	=	freestream

Introduction

LIQUID injection into supersonic streams has several practical applications. One prominent example is fuel injection in the combustor of an aerospace plane in the lower range of flight Mach number ($M_\infty < 8$). For the purpose of achieving the hypersonic flight of this vehicle, a new generation of air breathing engine, i.e., Scramjet engine[1] is needed. Due to scramjet engine combustor velocity on the order of 3000 m/s, residence times of fuel in the combustor are on the order of 10^{-3}–10^{-4} s.[2] With such a high velocity and low residence time, fuel must mix with air and burn quickly to prevent the need for excessively long combustors.[3]

The main problems are the uniform distribution of liquid fuel jet over the flow cross section, the achievement of a high level of liquid fuel atomization, and greater penetration of the fuel jet into the flow. The quantity of fuel injected in the combustion chamber is limited by the stoichiometric ratio of components. In addition, controlling such parameters of the fuel injection system as the pressure and the area of the holes have some technological limitations. For example, the penetration of the jet plume depends on the momentum ratio of the injectant liquid to the freestream.[4] If the momentum of the injectant for a given mass flow is set very low by using large diameter injectors, e.g., a good penetration will not be obtained. Also, the liquid fuel will remain in the boundary layer if the boundary-layer thickness is very thick, so that a good fuel-air mixture is not obtained.[5]

In order to achieve high penetration and a good air-fuel mixture, we have developed an improved bubbling jet system extending the ideas in Ref. 6. It was reported earlier that both the spray cone angle and the penetration height increased by using a bubbling jet system.[6] We have also clarified the liquid atomization process, the shock wave—bubbling liquid jet interactions, and the ability of controlling the penetration height and the mass flow rate.[7] For the next step, we use multiple injectors to get a total large mass flow using a small orifice. Therefore, the aims of this article are to clarify the flow patterns of multiple liquid injections into a supersonic flow and the effect of a bubbling jet on multiple liquid injections.

Experimental Procedure

Test Facilities

The data for this study are obtained in the 23- × 23-cm blowdown supersonic wind tunnel at Virginia Tech. This tunnel provides run times of about 15 s at a freestream Mach

Received Jan. 14, 1992; presented as Paper 92-5060 at the AIAA 4th International Aerospace Planes Conference, Orlando, FL, Dec. 1–4, 1992; revision received Aug. 10, 1993; accepted for publication Sept. 2, 1993.

*Visiting Research Scholar, Department of Aerospace and Ocean Engineering; also Associate Professor, Department of Mechanical Systems Engineering, Muroran Institute of Technology, Muroran, Hokkaido 050, Japan. Senior Member AIAA.

†W. Martin Johnson Professor and Department Head, Department of Aerospace and Ocean Engineering. Fellow AIAA.

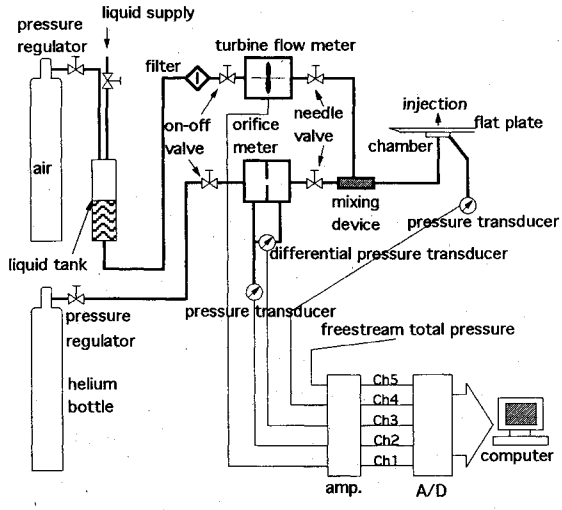

Fig. 1 Outline of experimental and measuring systems.

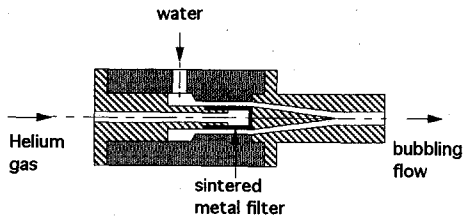

Fig. 2 Microbubble mixing device.

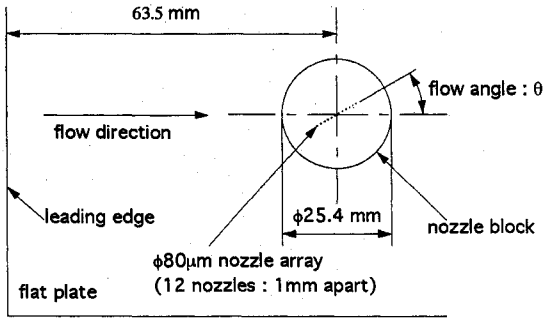

Fig. 3 Flat plate model.

number of 2.4, with a total temperature of 291 K and a total pressure of 4.5 atm. The wind tunnel is computer operated and controlled, resulting in accurate and repeatable runs. The total pressure $P_{t\infty}$ is maintained at ± 0.05 atm from run to run. The computer system also controls a 12-bit A/D data-acquisition system to sample and record various test parameters. Figure 1 shows outline of the experimental and measuring systems.

Injectant

Water was used to simulate a hydrocarbon fuel or liquid hydrogen. A 0.02–1% additive of surfactant was included in the water to reduce the surface tension and keep the bubble size small. The bubbling liquid of water and helium gas mixture was produced by using the mixing device as shown in Fig. 2. The mixing device was made from a sintered metal filter that consisted of 15-μm-diam stainless steel powder. The bubbling liquid was visually observed just coming out of the mixing device to get good mixtures and fine bubbles.

Flat-Plate Model

The bubbling liquid was injected through a flat plate having dimensions 15.24 × 22.86 × 0.95 cm and a sharp leading edge. A circular nozzle block that contained 12 circular injectors was located 6.35 cm downstream of the leading edge as shown in Fig. 3. Each of the 12 injectors had an orifice of 0.08 mm diam, and were 1.02 mm apart. The nozzle block could rotate. Therefore, the angle between the freestream and the orifice array (θ) was able to be set freely. The intent of this research was to simplify this flow problem as much as possible by studying a basic configuration that could later be extended. Also, the flat plate model was used to minimize the boundary-layer size and its effects.

Photographic Method

Two types of photographs were taken. First, a Nanopulse Lamp was used as the light source to take shadowgraphs. The 30×10^{-9} exposure time with type 57 Polaroid (ASA 3000) film provided instantaneous shock shape and side views of the liquid jet. Second, front-lighted photographs provided top views of the jet. Exposure times of 2×10^{-3} s were used on ASA 400 or 1000 film with a 35-mm camera.

Test Matrix and Parameters

In the present study, the experiments were performed at two major conditions, i.e., the constant supply pressure condition (P_j = 20–22 atm), and the constant liquid mass flow rate condition ($\bar{q}_l$ = 3–5). The angles between the orifice array and freestream direction (θ) of 0, 25, and 90 deg were tested. The resulting penetration and width of the jet plume were measured at 10-mm downstream position after the 12th orifice (corresponding to x/d much greater than 30).

Results and Discussion

Multiple Liquid Jets

Figure 4 shows a typical photograph of the multiple liquid jet injection transverse to a supersonic flow of M = 2.4 for the flow angle θ = 0 deg (parallel arrangement), and $\bar{q} \approx 13$ ($p_j \approx 22.8$ atm). The flow direction is from left to right, the plate is at the bottom and injection is up. The water included 1% additive of surfactant. It can be seen that the penetration of the jet array increases gradually from front to back. The last jet (12th jet) has over 5 times the penetration of the first one. The second jet penetrates in the wake behind the first jet so that it has greater penetration than that of the first one. Jets 3–12 also have the same situation. All of the jets just coming out of the orifice have a straight and very slender plume. Figure 5 shows the penetration of the jet plume measured directly from the photo of Fig. 4. The first jet has about h/d = 17 for the penetration height, and the last one

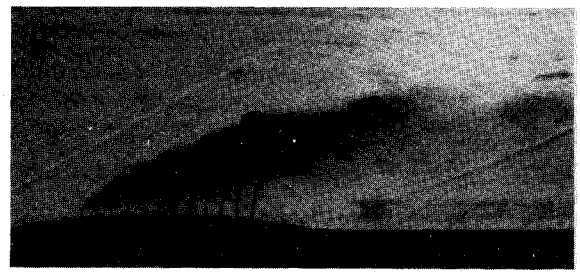

Fig. 4 Typical side view of multiple jet injection [no gas (γ = 0), $\bar{q}_l \approx 13$, $P_j \approx 22$ atm].

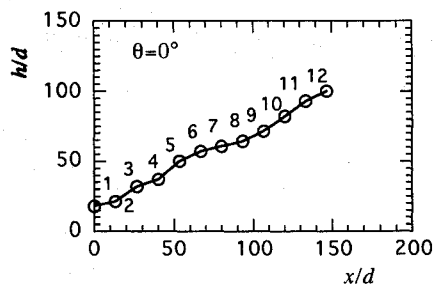

Fig. 5 Penetration of multiple jet injection [no gas (γ = 0), $\bar{q}_l \approx 13$, $P_j \approx 22$ atm, d = 0.08 mm].

has about $h/d = 100$. Our previous work[7] (using a single jet) reported that it had about $h/d = 20$ for the case of $\bar{q} = 13$. The first jet has almost the same value of penetration as the previous result,[7] while the last one has over 5 times the penetration of the result of the single jet case.

Figure 6 shows the resulting penetration at the 12th jet in the multiple jet plume with no gas conditions vs $\bar{q}$. The straight line in the figure indicates the best fit line with a power law, and the exponent is 0.475. This value is very close to the previously reported value of 0.5. Therefore, it seems that the resulting penetration of multiple jets is also approximately proportional to $\bar{q}$.[0.5]

Effect of Adding Microbubbles

General

Figure 7 shows the side view photograph of multiple injection for the case of $\gamma = 0.01$ and injection pressure of 22 atm, the same as that of Fig. 4. Comparing Fig. 7 with Fig. 4, the penetration of the jet plumes was reduced by adding the bubbles. That is different from the single injection case. For the single injection case, the penetration of the jet plume doesn't change with adding the gas at the constant supply pressure condition.[6,7] Observing both photographs of Fig. 4 and Fig. 7 in detail, each first jet seems to have the same penetration height of $h/d \approx 20$. While, for the bubbling jet, the second jet and the jets after the second have a smaller penetration than that of liquid-only jet, because the wake produced by each bubbling jet plume had a higher velocity field than that of the liquid-only jet. The 2nd and 12th jet have a straight plume, but the other jets have a conical plume. Therefore, it seems in this case that the bubbles were intermittent, resulting in an unstable jet with a conical plume.

Effect of γ on Side View Flow Pattern

Figures 8 and 9 show the flow pattern of the larger γ case ($\gamma \approx 0.02$ and 0.03) for the same injection pressure of Figs. 4 and 7. It can be seen that the penetration of the bubbling jet plumes decreases with increasing γ, because the wake behind the jet plume becomes weaker than that of smaller γ cases. In the cases of Figs. 8 and 9, all the jets have a conical plume. Thus, the microbubbles are coming continuously, so that good mixture was obtained. The conical shape plume suggests an increase of the width of the jet plume.

Observing Fig. 8 in detail, the atomized liquid particle flow after the multiple injections goes down to the boundary layer at about 8 mm after the 12th injector. The same flow pattern can be seen in Fig. 9. This means, we assume, that there is

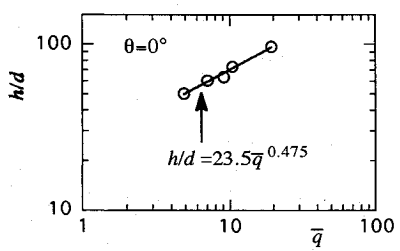

Fig. 6 Relation between h/d and $\bar{q}$ (no gas condition).

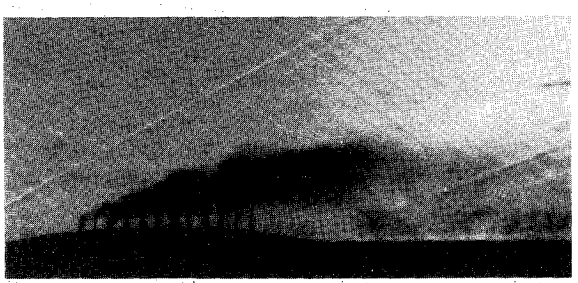

Fig. 7 Side view of multiple bubbling jet injection ($P_j \approx 22$ atm, $\gamma \approx 0.01$).

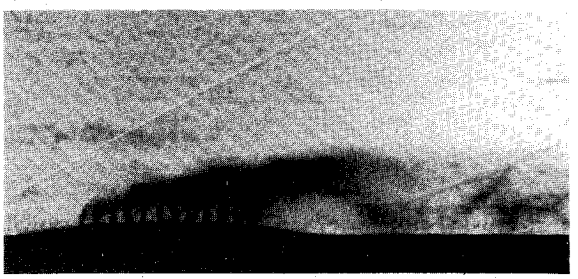

Fig. 8 Side view of multiple bubbling jet injection ($P_j \approx 22$ atm, $\gamma \approx 0.02$).

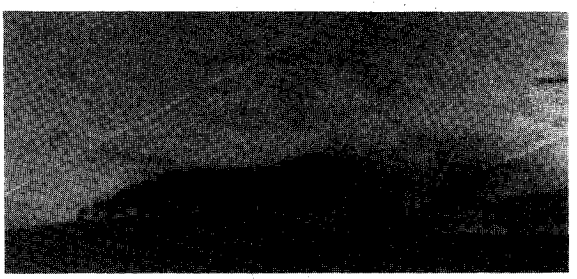

Fig. 9 Side view of multiple bubbling jet injection ($P_j \approx 22$ atm, $\gamma \approx 0.03$).

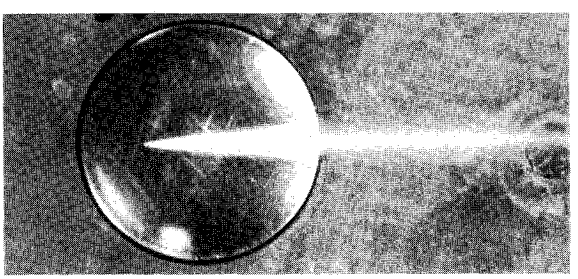

Fig. 10 Top view of multiple jet injection [$\dot{m}_l = 0.124$, $P_j \approx 4.1$ atm, g/s, $\gamma = 0$ (no gas), $\bar{q}_l \approx 3$].

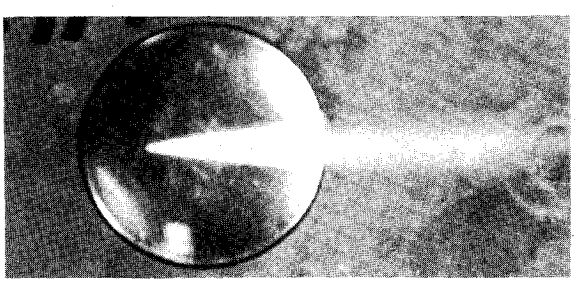

Fig. 11 Top view of multiple jet injection ($\dot{m}_l = 0.131$ g/s, $P_j \approx 8.9$ atm, $\gamma \approx 0.01$, $\bar{q}_l \approx 3$).

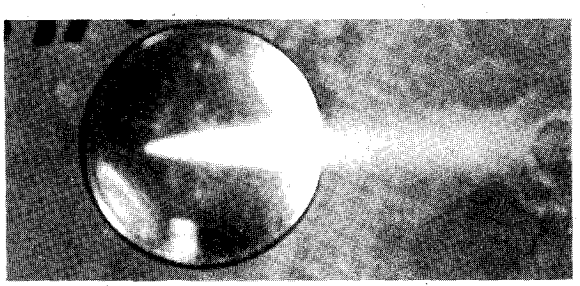

Fig. 12 Top view of multiple jet injection ($\dot{m}_l = 0.139$, $P_j \approx 19.6$ atm, $\gamma \approx 0.02$, $\bar{q}_l \approx 3$).

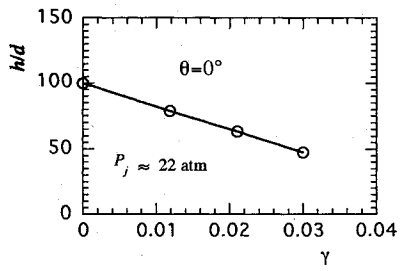

Fig. 13 Effect of γ on penetration for constant supply pressure condition.

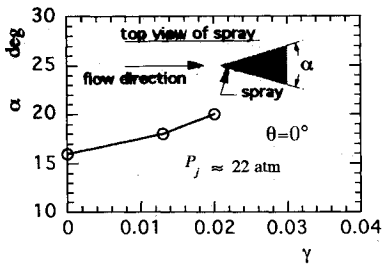

Fig. 14 Effect of γ on spray angle for constant supply pressure condition.

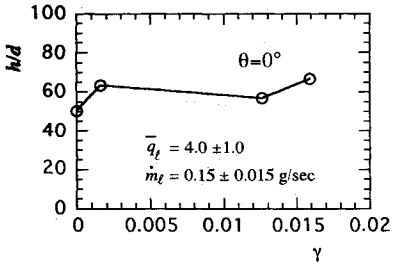

Fig. 15 Effect of γ on penetration for constant liquid mass flow rate condition.

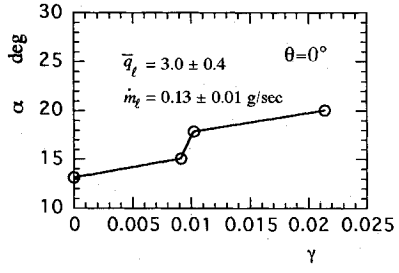

Fig. 16 Effect of γ on spray angle for constant liquid mass flow rate condition.

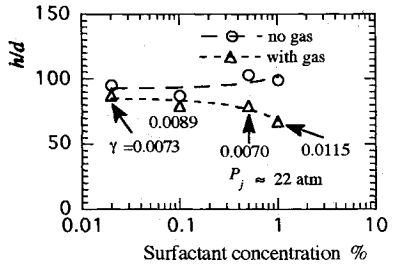

Fig. 17 Effect of surfactant concentration on penetration for constant supply pressure condition.

a recirculation area after the 12th jet. Therefore, this flow pattern including the recirculation area could be used as a flame holder.

Effect of γ on Top View Flow Pattern

Figures 10–12 show the top view of the multiple injections of $\gamma = 0$, $\gamma \approx 0.01$, and $\gamma \approx 0.02$ cases, respectively, for a constant liquid mass flow rate condition. It is seen that the width of the jet plume increases with increasing γ. For a constant supply pressure condition, the width of the jet plume also increased with increasing γ.

Effect of γ on Penetration and Spray Angle

Figures 13 and 14 show the resulting penetration height h/d vs γ and spray angle vs γ, respectively, for a constant supply pressure condition. The penetration height decreases from about 100 to 50, but the spray plume spreading angle increases 16–20 deg with increasing γ from 0 to about 0.02. Figures 15 and 16 also show the resulting penetration height h/d vs γ and spray angle vs γ, respectively, for a constant liquid mass flow rate condition. In this case, the penetration increased a little with increasing γ. The spray angle α increased from 13 to 20 deg, the same as the constant supply pressure condition case.

Effect of Concentration of Surfactant

Figure 17 shows the effect of the concentration of the surfactant on the penetration of the jet plume. The symbols ○ and △ mean the case of liquid jet and bubbling jet of $\gamma \approx 0.01$ (0.007–0.012), respectively. The penetration of the liquid-only jet showed almost no change as the concentration of the surfactant varied. The penetration of the bubbling jet decreases with increasing concentration of the surfactant. The increase of the amount of the surfactant, i.e., the decrease of surface tension of the liquid, creates a good bubbling flow, including fine bubbles. Then, the conical jet plume is obtained, so that the wake after each jet plume becomes weak and the penetration of the jet plume decreases.

For a 0.02% surfactant case, the bubbling jet has a straight column and/or a conical plume with small angle as shown in Fig. 18. For a 1% surfactant case, as mentioned before, most of the jets have a conical plume with a wide angle. Therefore, the decrease of the surface tension gives a good bubbling flow containing small bubbles.

Effect of θ on Flow Pattern

Figure 19 shows the side view photograph of liquid-only jet for the case of a flow angle of 90 deg and $\bar{q} = 13.7$. It has about $h/d \approx 40$ at the position $x/d \approx 30$, which is twice the penetration obtained for the case of a single jet.[7] Figure 20 shows the photograph of bubbling jets for the same injection pressure as that of Fig. 16 and $\bar{q} = 10.1$, $\gamma = 0.009$. In this case, the bubbling jet has almost the same penetration height as that of liquid-only jet.

For a constant mass flow rate condition case, the penetration of the jet plume increases from $h/d = 16$ to 42 with increasing $\gamma = 0$ to 0.015, as shown in Fig. 21. This is qualitatively the same as a single jet case, but the value of penetration was larger than that of a single jet case. This suggests that the distance between the jets is one of the important parameters.

Figures 22 and 23 show the side view photograph of $\gamma = 0$ and $\gamma \approx 0.03$ for the flow angle of 25 deg at the same injection pressure, respectively. The flow angle of 25 deg is very close to the Mach angle of $M = 2.4$. It is seen that each jet has the same penetration. Thus, there is no effect of the interaction between oblique shock wave and jets, because the oblique shock wave generated by the injection might be very weak. It can also be seen for the bubbling jet case that the jet has a conical plume, but almost the same penetration as the liquid-only jet case.

Fig. 18 Side view of multiple bubbling jet injection for the case of lower concentration of surfactant (0.02%) ($P_j \approx 22$ atm, $\gamma \approx 0.01$).

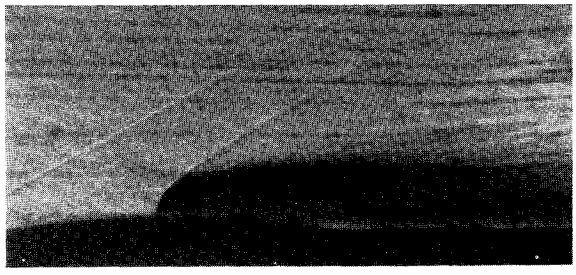

Fig. 19 Side view of multiple jet injection ($\theta = 90$ deg) ($P_j \approx 20$ atm, $\gamma = 0$).

Fig. 20 Side view of multiple bubbling jet injection ($\theta = 90$ deg) ($P_j \approx 20$ atm, $\gamma \approx 0.01$).

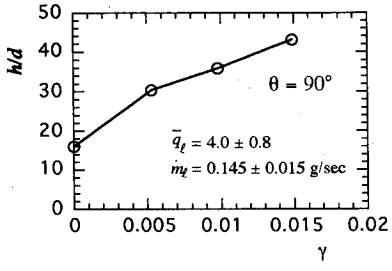

Fig. 21 Effect of γ on penetration for constant liquid mass flow rate condition ($\theta = 90$ deg).

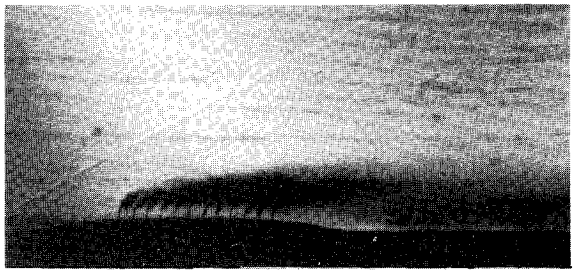

Fig. 22 Side view of multiple jet injection ($\theta = 25$ deg) ($P_j \approx 22$ atm, $\gamma = 0$).

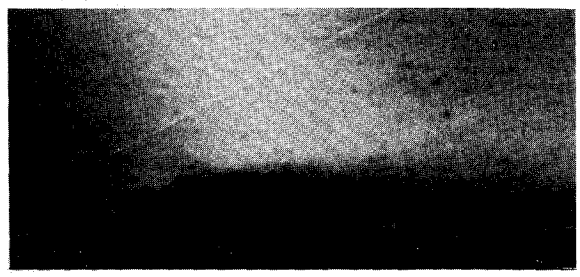

Fig. 23 Side view of multiple bubbling jet injection ($\theta = 25$ deg) ($P_j \approx 22$ atm, $\gamma \approx 0.03$).

Conclusions

Liquid and bubbling jets were injected from multiple injectors normal to a $M = 2.4$ airflow. The flow patterns were observed photographically. The penetration and width of the jet plumes were measured using nanoshadowgraphs and front-lighted pictures, respectively. The results are summarized as follows:

1) For the case of the parallel arrangement of the injector orifices to the airflow ($\theta = 0$ deg), the penetration of the jet array increased gradually from front to back. The last jet (12th jet) has over 5 times the penetration of the first jet for the liquid-only case.

2) For the bubbling jet case, the penetration of the first jet doesn't change with increasing γ at the constant injection pressure condition. The rear jets have less penetration height than that of liquid-only jet.

3) For the constant injection pressure condition, the resulting penetration of the jet plume decreased with increasing γ. On the other hand, for the constant mass flow rate condition, it increased a little with increasing γ.

4) Straight coherent jets just coming out of orifice were observed for the $\gamma = 0$ case. While conical jet plumes were obtained for the bubbling jet case. Therefore, the width of the jet plume increased by using the bubbling jet.

5) Each jet has the same penetration for θ of 90- and 25-deg cases.

6) As the amount of the surfactant increases, a good bubbling flow containing small gas bubbles was obtained. Then, we have a continuous bubbling jet.

7) The distance between jets is one of the more important parameters affecting the penetration for multiple jet injection in all angular arrangements of the array.

References

[1]Curran, E., and Stull, F., "The Potential Performance of the Supersonic Combustion Ramjet Engine," Technical Documentary Rept. Aeronautical Systems Division-TDR-63, 1963, pp. 1, 2.

[2]Swithenbank, J., "Hypersonic Air-Breathing Propulsion," *Progress in Aeronautical Science*, Vol. 8, 1967, pp. 229–294.

[3]Mays, R. B., Thomas, R. H., and Schetz, J. A., "Low Angle Injection into a Supersonic Flow," AIAA Paper 89-2461, July 1989.

[4]Baranovsky, S. I., and Schetz, J. A., "Effect of Injection Angle on Liquid Injection in Supersonic Flow," *AIAA Journal*, Vol. 18, No. 6, 1980, pp. 625–629.

[5]Arai, T., Sugiyama, H., Uno, N., and Takahashi, T., "Flow Characteristics of Atomizing Liquid Jet by Supersonic Flow and Related Shock Wave/Boundary Layer Interaction," *Proceedings of the International Conference on Liquid Atomization and Spray Systems-91* (Gaithersburg, MD), 1991, pp. 165–172.

[6]Avrashkov, V., Baranovsky, S., and Levin, V., "Gasdynamics Feature of Supersonic Kerosene Combustion in a Model Combustion Chamber," AIAA Paper 90-5268, Oct. 1990.

[7]Arai, T., and Schetz, J. A., "Penetration and Mixing of a Transverse Bubbling Jet into a Supersonic Flow," *Proceedings of the 2nd National Symposium on RAM/SCRAMJET* (Sendai, Japan), Feb. 1992, pp. 131–136.